The Structure of Surfaces

Editors: M.A.Van Hove and S.Y. Tong

With 223 Figures

Springer-Verlag
Berlin Heidelberg New York Tokyo

40. Competing Reconstruction Mechanisms in H/Ni(110)

R.J. Behm, K. Christmann, G. Ertl, V. Penka, and R. Schwankner
Universität München, D-8000 München 2, FRG

The mechanisms of the hydrogen-induced reconstructions of Ni(110) have been investigated. Below ~180 K a (2 × 1) lattice gas structure with $\theta_H = 1.0$ transforms into a 2D-(1 × 2) structure during addition of hydrogen up to $\theta_H = 1.5$. The phase transition, which involves a reconstruction of the surface, exhibits first-order behavior with no apparent activation energy. In contrast, at T > 180 K and already at low coverages, an activated, local transformation into a more stable 1D structure ('streaked structure') occurs. A lattice distortion to optimize the local metal structure with respect to the metal-adsorbate bond and thus increase the binding energy is introduced as a general model for many such adsorbate-induced surface phase transformations.

40.1 Introduction

Considerable work has been performed to investigate the structure and thermodynamic stability of ordered surface phases [40.1]. Especially for reconstructed surface phases, little is yet known about the microscopic mechanism and driving force of the phase transformation. For the system H/Ni(110), we have found two competing adsorbate-induced surface reconstruction mechanisms [40.2]. A full report will be published elsewhere, including a detailed description of the apparatus and the methods applied to meet the stringent requirements for surface cleanliness [40.3]. A brief overview of the main features of this adsorption system is first presented.

Exposure of the clean surface to H_2 at 120 K leads to the formation of a continuous sequence of ordered lattice gas structures from adsorbed H atoms, which are completed by a "(2 × 1)p1g1" structure, denoted below as (2 × 1), at $\theta_H = 1.0$ [40.4]. In this coverage range He scattering [40.5], LEED structure analysis [40.6] and EELS [40.7] indicate the occupation of quasi-threefold adsorption sites for the H atoms in zigzag rows along the [1$\bar{1}$0] direction. Beyond this coverage the LEED pattern of the (2 × 1) coexists with that of a reconstructed (1 × 2) phase [40.2,3], here denoted (1 × 2), until at saturation ($\theta_H = 1.5$) the whole surface is converted into the (1 × 2). The indicated coverage assignments were recently confirmed by nuclear microanalysis [40.8].

In contrast, annealing a surface exposed to H_2 at T > 180 K or exposure at T > 180 K leads to the irreversible formation of a structure which exhibits considerable disorder in the [001] direction. In the LEED pattern streaks between the integral order beams in [01] direction are observed. The saturation coverage in this structure is roughly similar to that in the (1 × 2) [40.3,8]. The structure itself is stable and only removed by H_2 desorption.

40.2 Results

The formation of the (1 × 2) reconstructed phase from the unreconstructed (2 × 1) was followed by monitoring the intensity of the (0, 3/2) beam as a function of H_2 exposure. In Fig.40.1c also the decay of the (1/2, 1) beam, related to the (2 × 1), and the behavior of the integral order (1,0) beam is displayed. The maximum in the (1/2, 1) beam served to define the coverage $\theta_H = 1$ at this point [40.5]. These data allow the following two conclusions. The (1 × 2) grows as islands in the surrounding 'sea' of (2 × 1) and the onset of intensity in the (0, 3/2) beam is always delayed by ca. 0.05 L with respect to the maximum in the (1/2, 1) beam. The island growth mechanism is evident from the relationship between the (1/2, 1) and the (0, 3/2) intensity. At all coverages between $\theta = 1.1$ and $\theta = 1.45$ the sum of the two normalized intensities I/I_{max} is constant, a clear indication of coexisting, rather large islands.

The delay between the maximum in the (2 × 1) intensity and the first appearance of the (1 × 2) might suggest nucleation of the latter phase at a critical coverage, i.e., supersaturation of the (2 × 1) phase at $\theta_H > 1.0$. This has been ruled out, however, by measurements of the diffuse elastic background and the beam profiles in the [10] and [01] directions, as indicated in Figs.40.1b,c. The intensity of the diffuse elastic background is related to the number of uncorrelated point defects and vibrationally induced displacements in the lattice. Since the temperature in these experiments was kept constant, changes in the latter can be neglected unless new phonon modes appear. Statistically distributed H atoms in the (2 × 1) would present a typical example of point defects, so they should therefore lead to a possibly temporary increase in the diffuse elastic background. However, the background intensity monitored in the 'windows' 1 and 2 in the reciprocal lattice as indicated in Fig.40.1b remains at a constant level as θ_H increases from 1 and starts to grow only around $\theta = 1.25$. Obviously more random defects are created once the (1 × 2) starts to cover major parts of the surface, e.g., by island coalescence, at $\theta_H \geq 1.25$.

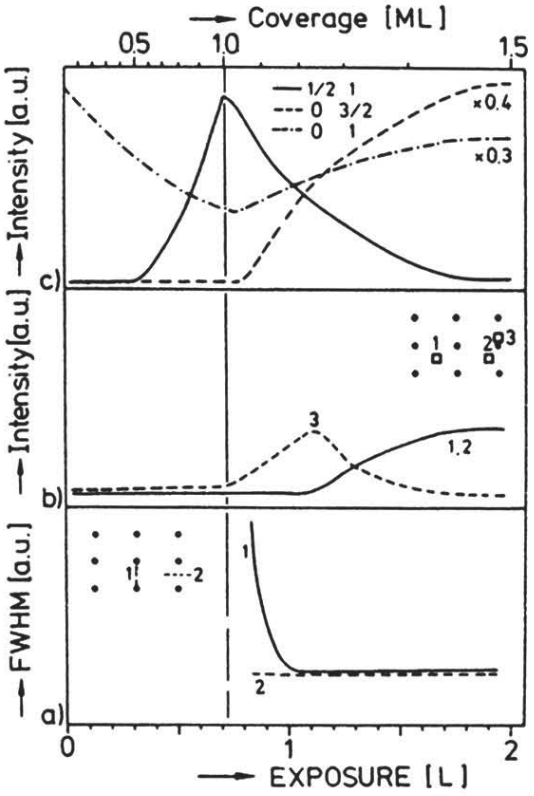

Fig.40.1. LEED during exposure to H_2 at 120 K: (*a*) profile width (FWHM) of (1, 1/2) beams as indicated; (*b*) diffuse background as indicated (*c*) integral intensity as indicated

If, in contrast, the delay in the appearance of intensity in the (1 × 2) related beams were caused by the initial formation of very small nuclei of (1 × 2), which subsequently grow, initially broad profiles of the (1, 1/2) beam in one or both directions should be observed, depending on the shape of these nuclei. In 'window' 3 the intensity between the (1, 1/2) and (1, 0) spot was monitored, where at higher temperature the streaks are formed. Curve 3 in Fig.40.1b clearly demonstrates that there is an intensity increase in this region right at the maximum of the (2 × 1), thus confirming this hypothesis.

The evaluation of the beam profiles supports this conclusion. The integral order (1,0) beam does not change its shape over the entire exposure range. The FWHM of the (1/2, 1) beam reaches the instrumental resolution, given by the instrumental response function, in both directions at $\theta = 0.96$ and remains there until at around $\theta = 1.4$ when the intensity is too low for further evaluation. The corresponding behavior of the FWHM of the (0, $\bar{1}$/2) beam is illustrated by the full line in Fig.40.1a. As soon as it can be evaluated around $\theta = 1.05$, the width of the profiles in the [10] direction is within the instrumental resolution. In the normal [01] direction, measured on the (1, $\bar{1}$/2) beam, the FWHM is clearly larger: initially, at $\theta = 1.05$, the measured width is about double the size of that in the [10] direction. With increasing coverage the width rapidly decreases and at $\theta = 1.15$ it also reaches its final value, close to the instrumental resolution.

These results indicate that the reconstructed (1 × 2) grows as islands in the surrounding (2 × 1), starting immediately when the (2 × 1) is fully developed. There is no indication for a supersaturation effect in the sense that H atoms might be statistically squeezed into the (2 × 1) without locally initiating the reconstruction as small islands of (1 × 2). Initially the (1 × 2) islands are elongated in the [1$\bar{1}$0] direction, with a rather small diameter in the [001] direction. The instantaneous formation of the (1 × 2) suggests that the reconstruction is not activated, which is supported by the results of similar LEED intensity measurements at temperatures between 120 K and 250 K [40.3].

The second reconstruction path leads to the 'streaked' structure, characterized by a LEED pattern in which the half-order spots of the (1 × 2) are elongated to streaks in the [01] direction. The energy and coverage dependence of the spot profiles also indicate an island growth mechanism although the islands exhibit inherent disorder. This structure is formed upon H adsorption at $T > 180$ K, independent of coverage and with a rather low critical coverage (< 5% at 300 K) [40.3], or upon annealing a hydrogen adlayer to $T > 180$ K. This transition *always* starts from the unreconstructed Ni surface, since the transformation from the reconstructed (1 × 2) into the streak phase proceeds through an intermediate, unreconstructed (1 × 1) Ni surface and partial loss of hydrogen [40.2].

This reconstruction proceeds rather slowly. To determine a possible activation barrier, a fixed amount of hydrogen was adsorbed at a low temperature which then was raised in a step and kept at the new value. The formation of the 'streaked' phase was monitored by LEED as a function of time. The rate of transformation (assumed to follow first-order kinetics) can be expressed as

$$\frac{dA_{str}}{dt} = A_{1\times1} \cdot \nu \cdot \exp(-E^*/R \cdot T) \quad ,$$

where A denotes the fraction of the surface existing in the respective phase, ν and E^* are the preexponential and the activation energy for the reconstruction. The activation barrier can be extracted from an Arrhenius plot of the integral intensities of the streaks, since for an island growth mechanism of the 'streaked' phase $A_{str} \sim I_{str}$. Analyzing the initial slopes of the intensities in this way yielded $E^* \simeq 50$ kJ/mole. In other experiments we verified that this activation energy for reconstruction also limits the adsorption rate of hydrogen at $T > 300$ K [40.3].

40.3 Discussion

The energetic situation for H/Ni, derived from thermal desorption and other data [40.3] is displayed in Fig.40.2. In the insert in the upper part the potential energy (per mole of adsorbed H_2) of the different adsorbed structures is indicated. The zero level of the energy scale corresponds to the clean unreconstructed Ni(110) surface and H_2 in the gas phase. The 'streaked' structure is more stable than H adsorbed on the (1 × 1) by 16 kJ/mole, but is separated by an activation barrier of 50 kJ/mole. The (1 × 2), however, is less stable: its net adsorption energy is only 64 kJ/mole, as outlined below.

The effect of increasing coverage becomes clearer from the main part of Fig.40.2 which shows a plot of the *integral* energy of the system as a function of coverage using the same zero level. Adsorption on the (1 × 1) surface [and (2 × 1) formation] leads to a continuous energy decrease, whose slope corresponds to the differential adsorption energy of 71 kJ/mole [40.3]. This phase obviously cannot accommodate more than one monolayer of hydrogen, which is reached in point A. Further uptake, which still leads to an energy gain of the system, is possible only by forming the reconstructed (1 × 2). During this process the (2 × 1) is locally converted into (1 × 2), a measured adsorption energy thus includes a contribution to raise the energy level of those H atoms already adsorbed on the (1 × 1)-Ni surface, e.g., in the (2 × 1). Since the adsorption is not activated, this adsorption energy is identical to the activation energy for desorption from the (1 × 2) of 51 kJ/mole [40.3], which gives the slope of the line A-B. The net adsorption energy of the (1 × 2) [H adsorption and displacement of the Ni atoms into the (1 × 2)] is given by the slope of the dashed line O-B corresponding to 64 kJ/mole. The adsorption energy of the 'streaked' structure, symbolized by the dash-dotted line, is constant up to medium coverages at 87 kJ/mole and decreases at higher coverages, due to occupation of less favorable sites and/or repulsion between the adsorbed atoms [40.3].

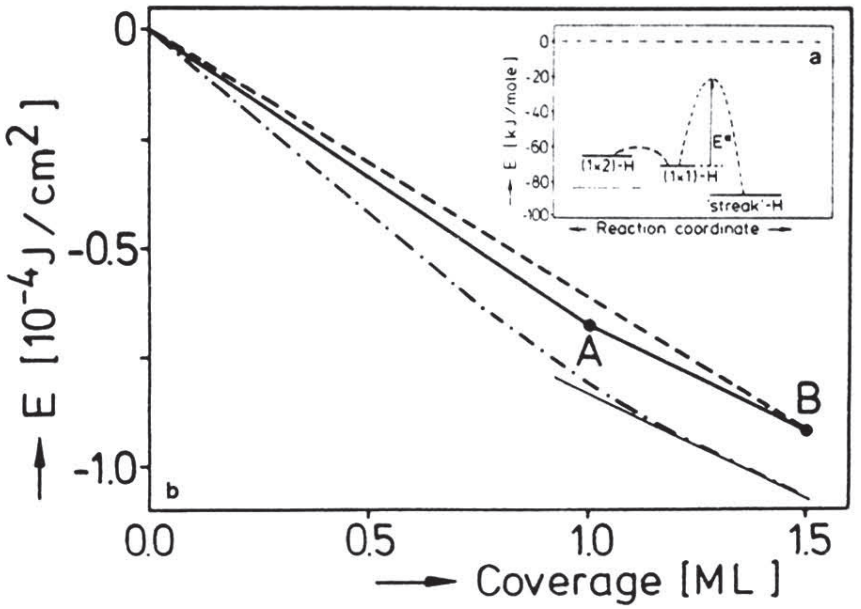

Fig.40.2. Potential energy diagram. (*a*) (Differential) adsorption energies and activation barriers of the respective reconstruction; (*b*) (integral) system energy [Ni(110) + H_2] as f(θ) for the different stru tures: (----) (imaginary) H/(1 × 2); (O——A) H/(1 × 1) (A——B) coexisting H/(1 × 1 and H/(1 × 2); (—·—·—) H/ 'streaked' structure

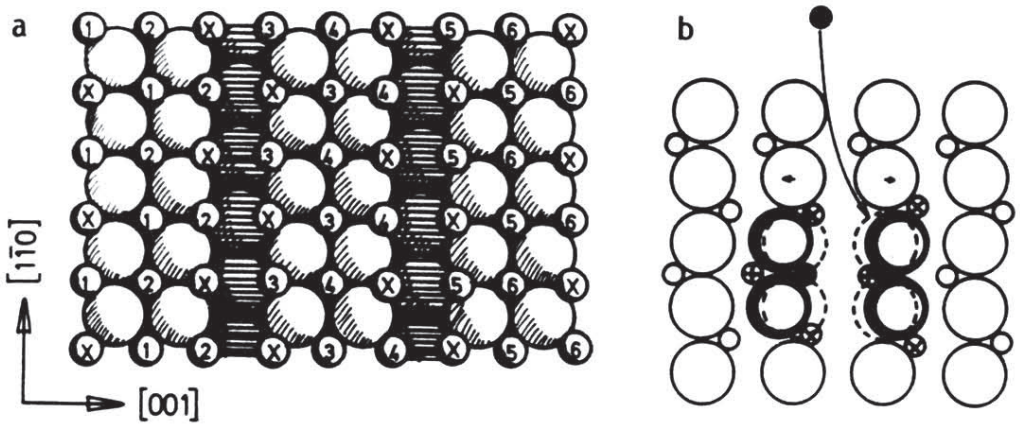

Fig.40.3. (**a**) Structure model of the (1 × 2): ○: Ni atoms in the 1st layer (●: 2nd layer); ○: H atoms, 1-6: zigzag rows in the former (2 × 1); x: additional H atoms. (**b**) Mechanism for the (1 × 1) ⇌ (1 × 2) reconstruction): ○: Ni atoms (**O**: reconstructed); ○ ⊕ ⊗: H atoms in the (2 × 1), position I, position II; ●: 'additional' H atoms to nucleate the (1 × 2)

With respect to the microscopic mechanism the data show that the (1 × 2) forms from the (2 × 1) without any noticeable supersaturation. In other words, the free enthalpy of a nucleus of (1 × 2) in a surrounding of (2 × 1) has its maximum already at a very small size and any further growth leads to a stabilization of the cluster [40.9]. Figure 40.3 illustrates a possible mechanism which would fulfill this requirement. The open dots represent H atoms in a (2 × 1) structure on the unreconstructed Ni surface. Uptake of an additional H atom (filled dot) with an adsorption energy E_{ad} causes local displacement of neighboring Ni atoms (ΔE_{rec}), as depicted. The adsorption energy of the neighboring H atoms is affected by the movement of the underlying Ni atoms ($\Delta E'_{ad}$ for H atoms in position I, $\Delta E''_{ad}$ for those in position II) and by (presumably repulsive) lateral interactions with the addition H atom (E_{aa}). The change in total energy for this nucleus can then be written as

$$E_\Lambda = -E_{ad} + 4 \cdot \Delta E_{rec} + 3 \cdot \Delta E'_{ad} + 4 \cdot \Delta E''_{ad} + 4 \cdot E_{aa} \quad . \tag{40.1}$$

Growth of the nucleus by adsorption of a second H atom, as indicated by the arrow, will lead to the following energy balance:

$$E_2 = -2 \cdot E_{ad} + 6 \cdot \Delta E_{rec} + 4 \cdot \Delta E''_{ad} + 8 \cdot E_{aa} \quad , \tag{40.2}$$

resulting in a stabilization of one 2-H cluster as compared to two 1-H clusters by

$$\Delta E = 2E_1 - E_2 = 2 \cdot \Delta E_{rec} + 4 \cdot \Delta E''_{ad} \quad . \tag{40.3}$$

Any further growth in the same lattice direction does not lead to an additional stabilization ΔE, barring more complicated interactions. The critical size of the cluster is thus reached already if one additional H atom is built into the (2 × 1) and locally displaces the surrounding Ni atoms. Growth in the [001] direction requires formation of a new, independent nucleus, which in turn can again easily grow in [1$\bar{1}$0] as is observed experimentally. This mechanism also predicts preferential one-dimensional growth in the [1$\bar{1}$0] direction which can formally be described as a collective phenomenon. The reconstruction will almost simultaneously affect long double rows of Ni in the [1$\bar{1}$0] direction and finally lead to the structure model of Fig.40.3a [40.2]. It is also obvious that the (2 × 1) will be a prerequisite for this mechanism.

The low observed activation barrier might be due to the fact that dissociation and subsequent chemisorption can take place at the same position and probably also simultaneously with the reconstruction. Therefore the energy gained by the former process can be used to overcome the barrier for reconstruction without any need for additional thermal activation.

In analogy the formation of the 'streaked' structure has to account for the increase in the net adsorption energy E with respect to that on the (1 × 1) and the observed activation barrier for its formation of ca. 50 kJ/mole. Thermal activation appears necessary, if the adsorbed particles have already completely accommodated before the reconstruction takes places. This agrees well with the experimental observation that hydrogen must first adsorb on the (1 × 1) surface ($\theta_{crit} \simeq 5\%$) before the reconstruction can start. The increase in the net adsorption energy E must be due to an increase in the term E_{ad}. The total contribution of the other terms —especially the lattice strain ΔE_{rec}— can then be calculated to be small for the 'streaked structure', but larger for the (1 × 2) by using the adsorption energies on Ni(111) and Ni(100) as an upper limit for E_{ad} [40.10]. Our structure model for the (1 × 2), Fig.40.3, indeed postulates occupation of comparable sites [40.2].

In analogy with bulk phase transformations [40.11] surface transformations are generally characterized as being 'displacive' (gradual displacement of surface atoms) or of 'order-disorder' type (e.g., phase transitions in lattice gas systems) [40.11]. Both mechanisms seem to apply for surface reconstruction: the temperature-dependent c(2 × 2) like reconstructions of Mo(100) and W(100) [40.13] are unanimously attributed to periodic lattice distortions (PLD) and therefore belong to the 'displacive' type, while for the (1 × 2) → (1 × 1) transformation of Au(110) there is evidence of an order-disorder mechanism [40.14]. The two H-induced surface reconstructions on Ni(110) are clearly 'displacive'. Because of the island growth (i.e., constant local θ_H) a constant (not gradual) Ni displacement is expected.

The driving force for the H/Ni surface reconstruction can be identified as the gain in potential energy $N \cdot E_{ad}$ (N = number of adsorbed particles), the first term in (40.1,2). This energy gain may result from an increase in adsorbate uptake (>N) as in the (1 × 2) or an increase of the differential adsorption energy E_{ad} as in the 'streaked' structure. This energy increase is sufficient to compensate for all other contributions, especially the energy necessary to reconstruct the surface, ΔE_{rec}. The proposed mechanism thus consists of a local distortion of the metal surface lattice to gain the most possible substrate-adsorbate interaction energy, while simultaneously keeping the energy loss due to the metal rearrangement as low as possible.

In contrast, for W(100) and Mo(100) the geometry of the Fermi surface, which causes charge density waves at the surface, was believed to be the origin of their reconstruction. In a recent calculation, however, a more local atom-pairing model comparable to a Jahn-Teller distortion is favored as the main energy source [40.15]. This energy gain due to variations in the electronic structure of the metal may occur also for the system H/Ni(110), but it is not expected to play a dominant role. A similar increase in the adsorption energy E_{ad} was recently demonstrated to be responsible for the CO-induced removal of the hexagonal reconstruction on Pt(100). In that case the term E_{ad} could be determined separately and was found to be 155 kJ/mole on the (1 × 1) and 113 kJ/mole on the hex surface [40.16].

In summary, the (1 × 2) is formed by a non-activated process. The total energy gain stems from a coverage increase, while the individual Ni-H bond is weaker. The formation of the 'streaked' structure is activated by ~50 kJ/mole. It is the most stable structure. The critical coverage for nucleation amounts to ⩽5% of a monolayer for the 'streaked' structure but is negligible for the (1 × 2). The proposed reconstruction mechanism accounts qualitatively for these features as well as for the preferential growth of the (1 × 2) in the [1$\bar{1}$0] direction, which simulates a collective effect. A local lattice distortion to maximize the Ni-H binding energy without creating too much strain for the Ni surface is suggested to be the energetic driving force. This model has characteristics which classify it as a displacive phase reconstruction, and is proposed as a general model for many other adsorbate-induced surface phase transformations.

Acknowledgment. We gratefully acknowledge P.R. Norton for information from [40.8] prior to publication and for valuable discussions. Financial support was obtained from the Deutsche Forschungsgemeinschaft (SFB 128).

References

40.1 L.D. Roelofs, P.J. Estrup: Surf. Sci. **125**, 51 (1983)
40.2 K. Christmann, V. Penka, R.J. Behm, F. Chehab, G. Ertl: Solid State Commun. (in press)
40.3 V. Penka, R.J. Behm, K. Christmann, G. Ertl, R. Schwankner: In preparation
40.4 V. Penka, K. Christmann, G. Ertl: Surf. Sci. **136**, 307 (1984)
40.5 K.H. Rieder, T. Engel: Phys. Rev. Lett. **43**, 373 (1979); **45**, 824 (1980); T. Engel, K.H. Rieder: Surf. Sci. **109**, 140 (1984)
40.6 W. Reimer, W. Moritz, R.J. Behm, G. Ertl, V. Penka: To be published
40.7 N.J. DiNardo, E.W. Plummer: J. Vac. Sci. Technol. **20**, 890 (1982)
40.8 T.E. Jackman, J.A. Davies, P.R. Norton, W.N. Unertl, K. Griffiths: Surf. Sci. **141**, L313 (1984)
40.9 B. Mutaftschiev (ed.): *Interfacial Aspects of Phase Transformations*, Nato Adv. Study Inst. Series, B (Reidel, Dordrecht 1982)
40.10 K. Christmann, O. Schober, G. Ertl, M. Neumann: J. Chem. Phys. **60**, 4528 (1974)
40.11 R.A. Cowley: Adv. Phys. **29**, 1 (1980)
40.12 R.F. Willis: In *Proc. Many Body Phenomena at Surfaces*, ed. by D.C. Langreth, D. Newns, H. Suhl (Academic, New York 1984)
40.13 R.A. Barker, P.J. Estrup: J. Chem. Phys. **74**, 1442 (1981); D.A. King, G. Thomas: Surf. Sci. **92**, 201 (1980) and references therein
40.14 D. Wolf, H. Jagodzinski, W. Moritz: Surf. Sci. **77**, 283 (1978)
40.15 I. Terakura, K. Terakura, N. Hamada: Surf. Sci. **111**, 479 (1981)
40.16 R.J. Behm, P.A. Thiel, P.R. Norton, G. Ertl: J. Chem. Phys. **78**, 7437, 7448 (1983)